Single-crystal Electron Spin Resonance Spectrum of Dichloro-oxobis(triphenylphosphine oxide)vanadium(IV), a Monomeric Oxovanadium(IV) Compound †

Brendan Gahan and Frank E. Mabbs *
Department of Chemistry, University of Manchester, Manchester M13 9PL

The single-crystal e.s.r. spectra of the title compound $[VOCl_2(OPPh_3)_2]$, at 298 K and *Q*-band frequencies, in the crystallographic *ab*, *bc**, and *ac** planes are reported. These spectra were interpreted by simulation, which involved diagonalisation of the matrix resulting from the axial spin Hamiltonian (i)

$$\mathcal{H} = \beta[g_{\parallel}H_z\hat{S}_z + g_{\perp}(H_x\hat{S}_x + H_y\hat{S}_y)] + A_{\parallel}\hat{S}_z\hat{I}_z + A_{\perp}(\hat{S}_x\hat{I}_x + \hat{S}_y\hat{I}_y) \quad \text{(i)}$$

and the assumption of a Gaussian line-shape function with linewidths composed of a Van Vleck truncated dipolar contribution plus an addition linewidth. The spin-Hamiltonian parameters which gave good simulations were $g_{\parallel} = 1.930 \pm 0.002$, $g_{\perp} = 1.974 \pm 0.002$, $A_{\parallel} = -(175.0 \pm 2.8) \times 10^{-4}$ cm^{-1}, and $A_{\perp} = -(66.1 \pm 2.8) \times 10^{-4}$ cm^{-1}. These parameters were used, in conjunction with the published electronic absorption spectrum, to derive the molecular-orbital coefficients in an empirical molecular-orbital scheme for the molecule.

The measurement of e.s.r. spectra of undiluted single crystals of *d*-transition-metal complexes can result in limited information being obtained, due to the many neighbouring magnetic dipoles interacting to such an extent that hyperfine structure is not observed.[1,2] Also, in undiluted crystals, magnetic exchange interactions between centres which are expected to be magnetically inequivalent may lead to the occurrence of only a single line, the position of which occurs at the mean resonance position of the two individual centres at that orientation.[1,3] This results in a loss of information concerning the orientations of the molecular *g* tensors. We are presently investigating the electronic structures of oxovanadium(IV) compounds, using electronic absorption [4] and e.s.r. spectroscopy. Although there have been many e.s.r. studies on oxovanadium(IV) systems these have mainly involved fluid or frozen solutions.[5] Work on dilute single crystals has been limited by the scarcity of isomorphous diamagnetic host lattices for oxovanadium(IV) compounds, although a few such studies have been reported.[6]

Recently the single-crystal e.s.r. spectra of undiluted $[VO(pbd)_2]$, where pbd = 1-phenylbutane-1,3-dionate, have been reported.[7] In this system magnetic exchange interactions of a similar magnitude to the vanadium hyperfine interaction, between centrosymmetrically related vanadium centres led to e.s.r. spectra with unusual line shapes, and to numbers of lines which did not correspond to the pattern expected from the interaction of the electrons with two vanadium nuclei. During the course of our investigations we have obtained the single-crystal e.s.r. spectra of a number of undiluted oxovanadium(IV) compounds. These spectra exhibit a variety of spectral patterns which have been interpreted on the basis of differing types of magnetic exchange interactions ranging from effectively monomeric systems, as in the present compound $[VOCl_2(OPPh_3)_2]$, to extended exchange throughout a crystal.[8] In the present context we use the term monomeric to describe those systems where any exchange interactions are insufficient to cause the appearance of extra features in the e.s.r. spectra, the only effects possibly being on the observed linewidths of the e.s.r. transitions. Thus for the present compound the *maximum* number of observed e.s.r. lines will be eight arising from the interaction of the unpaired electron with the nuclear spin of ^{51}V, $I = \frac{7}{2}$.

† *Non-S.I. unit employed:* G = 10^{-4} T.

Experimental

The complex was prepared by adding PPh_3 (1.3 g) to a solution of $VOCl_2$ (0.26 g) in dried CH_2Cl_2–CH_3CN (1 : 1, 50 cm^3). After *ca.* 30 min the pale green solution produced large green plates of $[VOCl_2(OPPh_3)_2]$ which were suitable for the e.s.r. study (Found: C, 62.5; H, 4.3; Cl, 10.4; P, 8.8; V, 7.3. Calc. for $C_{36}H_{30}Cl_2O_3P_2V$: C, 62.2; H, 4.3; Cl, 10.2; P, 8.9; V, 7.3%).

E.s.r. spectra were obtained on oriented (by standard *X*-ray techniques) single crystals, at *Q*-band frequencies, using a Varian E112 spectrometer, by methods previously described.[9] The single crystals were oriented such that spectra could be obtained in the crystallographic *ab*, *bc**, and *ac** planes. Spectra recorded at 298 K are shown in Figures 1—3. No significant variations were found when spectra were recorded in the temperature range 298—4.2 K. Variable temperatures were achieved using an Oxford Instruments ESR 35 continuous flow cryostat.

Results and Discussion

Experimental E.S.R. Spectra.—These were recorded in the crystallographic *ab*, *bc**, and *ac** planes and are shown in Figures 1—3 respectively. With the applied magnetic field parallel to the *c** axis the spectrum consisted of an equally spaced eight-line pattern in which the lines were of almost equal peak-to-peak height, as would be anticipated for a monomeric oxovanadium(IV) species. However, when the applied magnetic field is moved away from *c** in either the *bc** or *ac** planes the relative peak-to-peak heights within a spectrum change. At some orientations eight features are no longer clearly observed (for example when the applied magnetic field is parallel to the *b* axis), giving spectra quite untypical of that expected from a monomeric oxovanadium(IV) species.

The magnetic field at the centre of the spectral pattern and the total spectral width remain approximately unchanged for all orientations of the magnetic field in the *ab* plane. The *ab* plane corresponds closely to the molecular *xy* plane (see below). In the *bc** and *ac** planes the magnetic field at the centre of the spectral pattern and its total width are at a maximum when the magnetic field is parallel to *c** and decrease as the applied field moves towards *b* or *a*, at which orientations

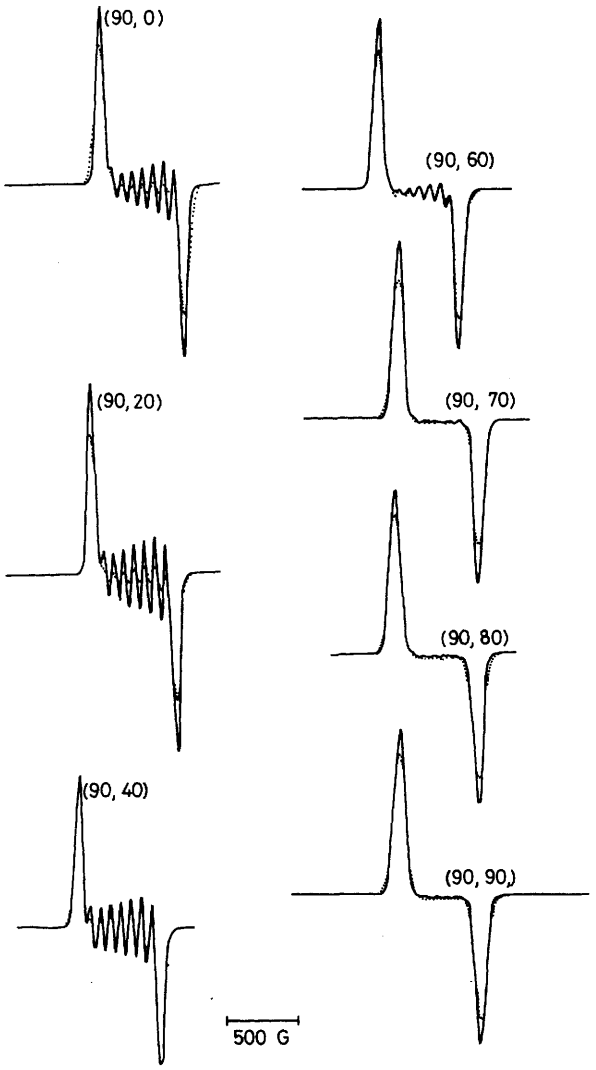

Figure 1. E.s.r. spectrum at 298 K recorded in the *ab* plane. ——, Experimental; · · · ·, simulated where different from experimental. See text for parameters used in the simulations, and for the orientation of the applied magnetic field, (η,γ), with respect to the crystal

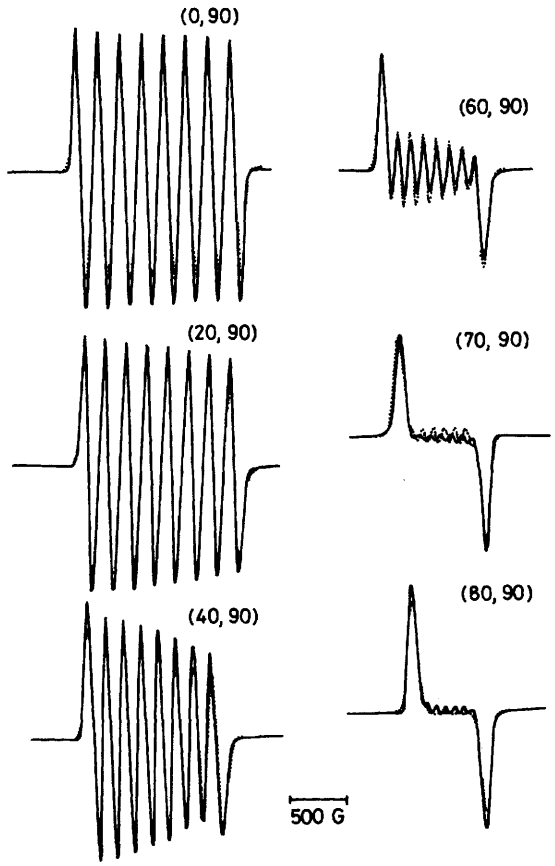

Figure 2. E.s.r. spectrum at 298 K recorded in the *bc** plane. —— Experimental; · · · ·, simulated where different from experimental. See text for parameters used in the simulations

the centre and total width of the spectrum reach a minimum value. The *c** direction is close to the V–O terminal direction (see below).

Simulated E.S.R. Spectra.—Crystal and molecular structure. The complex $[VOCl_2(OPPh_3)_2]$ crystallises [10] in the monoclinic space group $P2_1/c$, with $a = 17.19(1)$, $b = 18.34(1)$, $c = 11.15(1)$ Å, $\beta = 98.67(5)°$, and $Z = 4$. The vanadium atom is five-co-ordinate with an approximately square-pyramidal co-ordination geometry. The terminally bonded oxygen atom forms the apex of the pyramid and the base of the pyramid consists of a pair of mutually *trans* chlorine atoms and a pair of mutually *trans* triphenylphosphine oxide ligands. The metal–ligand bond lengths were not very different to those previously reported for other oxovanadium(IV) complexes. Figure 4 shows the unit cell of $[VOCl_2(OPPh_3)_2]$ projected in the *ab* plane. Within the unit cell, the $[VOCl_2(OPPh_3)_2]$ molecules pack in two pairs, where the molecules within a pair are related by a centre of inversion, and molecules in different pairs are related by a two-fold rotation about the crystallographic *b* axis. The closest vanadium–vanadium separation is 8.8 Å between molecules related by a centre of inversion. In contrast to $[VOCl_2(tmu)_2]$ and $[H_2tmen][VO(mal)_2(H_2O)]\cdot 2H_2O$,† no extended chains or layers with comparable vanadium–vanadium separations are found in this structure.

Method of simulation. The $[VOCl_2(OPPh_3)_2]$ molecule possesses no crystallographically imposed symmetry, but by comparison with higher symmetry oxovanadium(IV) complexes [4] the molecular *z* axis was chosen to lie parallel to the vanadium–terminal oxygen bond direction. A preliminary analysis of the e.s.r. spectra indicated that the principal molecular *g* and *A* values were axially symmetric and, together with the low molecular symmetry of the complex, this made the choice of the molecular *x* and *y* directions rather arbitrary. The molecular *x* axis was chosen to be parallel to the projection of the nearest-neighbour vanadium–vanadium vector onto the plane perpendicular to the molecular *z* axis, as described by Belford and co-workers.[7] The direction of the molecular *y* axis was chosen to give a mutually orthogonal set of molecular axes. The vanadium–terminal oxygen bond direction lies within 6° of the crystallographic *c** axis and it transpired that the molecular *x* axis was close to the crystallographic *a* axis, whilst the molecular *y* axis was close to the crystallographic *b* axis. In the crystallographic *ab* and *bc** planes there should be two distinct, magnetically inequivalent sites in the unit cell, whereas in the *ac** plane all sites are magnetically equivalent. Although the individual e.s.r.

† See preceding papers for ligand abbreviations.

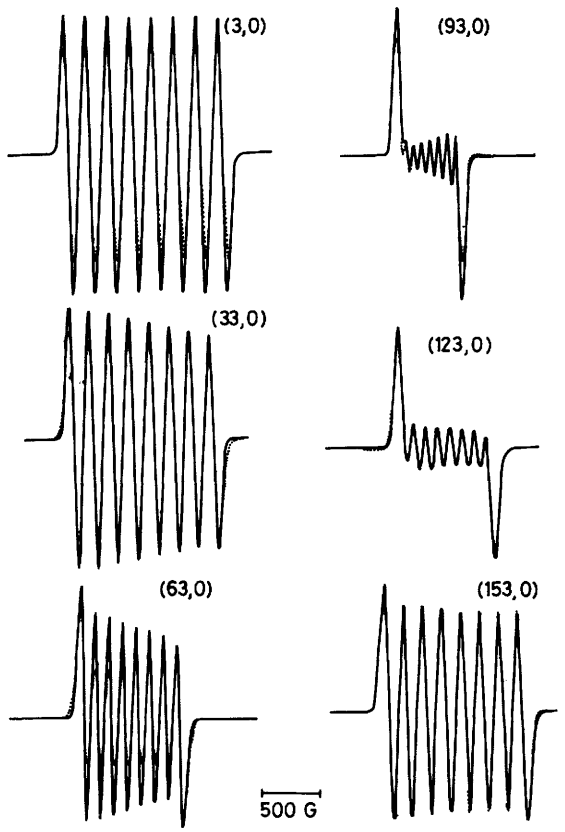

Figure 3. E.s.r. spectrum at 298 K recorded in the *ac** plane. Details as in Figure 2

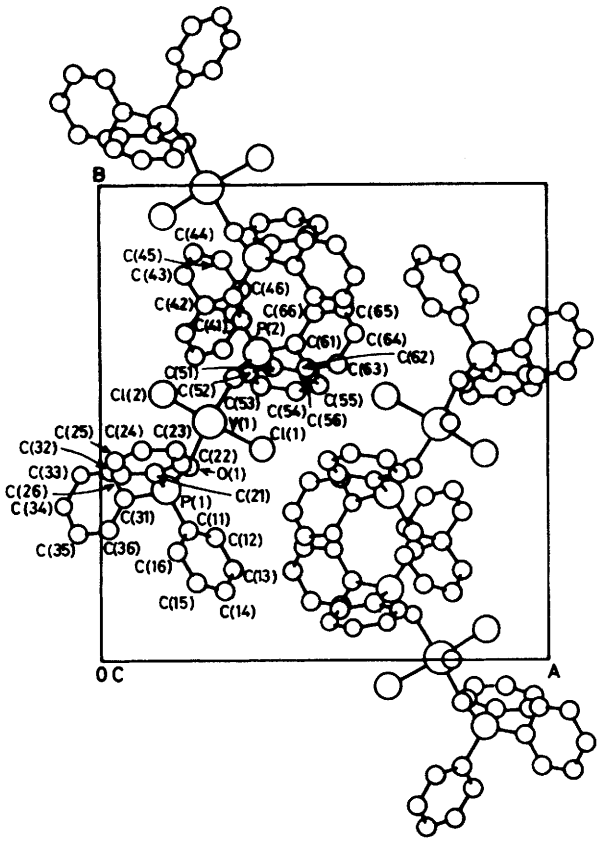

Figure 4. Unit cell of $[VOCl_2(OPPh_3)_2]$ projected in the *ab* plane

spectra from the inequivalent sites were not resolved in the *ab* and *bc** planes, it was necessary to calculate the spectrum from each site and to display the sum of these spectra as the final simulation.

The single-crystal e.s.r. spectra of $[VOCl_2(OPPh_3)_2]$ can be reproduced using a simple $S = \frac{1}{2}$, $I = \frac{7}{2}$ monomeric model. An adequate spin Hamiltonian for such a system, where the g and A tensors have principal axes which coincide with molecular axes, is given by equation (1) where θ and φ are

$$\mathcal{H} = \beta H(g_{xx}\hat{S}_x\sin\theta\cos\varphi + g_{yy}\hat{S}_y\sin\theta\sin\varphi + g_{zz}\hat{S}_z\cos\theta) + A_{xx}\hat{S}_x\hat{I}_x + A_{yy}\hat{S}_y\hat{I}_y + A_{zz}\hat{S}_z\hat{I}_z \quad (1)$$

the polar angles of the applied magnetic field, H, with respect to the molecular axes.

With e.s.r. measurements obtained in the *ab*, *bc**, and *ac** crystallographic planes, when the molecular axes do not coincide with the *a*, *b*, and *c** axes, then the direction of the applied magnetic field as applied to the crystal is related to the molecular directions by equation (2) where η is the

$$\begin{pmatrix}\sin\theta\cos\varphi\\ \sin\theta\sin\varphi\\ \cos\theta\end{pmatrix} = \begin{pmatrix}l_{xa} & m_{xb} & n_{xc}\\ l_{ya} & m_{yb} & n_{yc}\\ l_{za} & m_{zb} & n_{zc}\end{pmatrix}\begin{pmatrix}\sin\eta\cos\gamma\\ \sin\eta\sin\gamma\\ \cos\eta\end{pmatrix} \quad (2)$$

angle between H and c*, γ is the angle between *a* and the projection of H in the *ab* plane [the orientation of the applied magnetic field with respect to the crystal being expressed as (η,γ)], and l_{ij}, m_{ij}, and n_{ij} are the direction cosines of the molecular axis i with the crystallographic axis j.

The spectrum simulation at any orientation proceeded by diagonalising the 16 × 16 Hermitian matrix derived from equations (1) and (2) and the product functions $|m_S, m_I\rangle$, where $m_S = \pm\frac{1}{2}$ and $m_I = \pm\frac{7}{2}, \pm\frac{5}{2}, \pm\frac{3}{2}$, or $\pm\frac{1}{2}$ for ^{51}V. The input parameters to this matrix are the unknowns g_{xx}, g_{yy}, g_{zz}, A_{xx}, A_{yy}, and A_{zz} together with the calculated values of θ, φ, and H. The e.s.r. experiment involved sweeping the applied magnetic field at a fixed microwave frequency. In order to avoid diagonalising the matrix at a large number of magnetic fields we performed only one diagonalisation per orientation by calculating the resonance field for the effective g values at that orientation, equation (3) where $g_{eff.} = (g_{xx}^2\sin^2\theta\cos^2\varphi + g_{yy}^2\sin^2\theta\sin^2\varphi + g_{zz}^2\cos^2\theta)^{\frac{1}{2}}$. This approach will be valid only when second-order hyperfine effects are negligible, *e.g.* at *Q*-band, frequencies, and over restricted ranges of magnetic fields. However, our simulations indicate that they are valid for spectral widths up to *ca.* 2 000 G.

$$H = h\nu/g_{eff.}\beta \quad (3)$$

The matrix diagonalisation yielded eigenvalues and their associated eigenvectors. All possible differences between these eigenvalues were considered and converted into resonance magnetic field, H_R, and their transition probabilities calculated. The contribution to the first-derivative spectrum from each individual transition was calculated assuming a Gaussian line-shape function [11] [see equation (A36), ref. 8*b*]. The contribution from each transition was truncated for H_A more than $\pm 3\Delta B$ from H_R, where ΔB is the linewidth parameter. The total first-derivative spectrum, TS, was obtained from equation (4), where p = the number of magnetically inequivalent

$$TS = \sum_p \sum_{i=1}^{q} \sum_r \left(\frac{dI}{dH_A}\right)_i \quad (4)$$

centres at the orientation considered, q = the total number of transitions per centre, and r = the number of applied magnetic field points each separated by ΔH_A. ΔB was taken to be the sum of the two contributions ΔB_d and ΔB_m. The first of these arises from the dipolar interaction between a paramagnetic centre and all surrounding paramagnetic centres. It was calculated from the known crystallography and Van Vleck's truncated dipolar broadening equation,[12] see equation (A37) of ref. 8*b*. The second contribution ΔB_m was assigned as an additional linewidth which was found necessary for adequate simulation of the spectral profiles. The maximum excursion of the computed spectrum from the baseline was scaled to that of the experimental spectrum and the spectrum displayed on a Benson narrow-drum graph plotter.

The decision to simulate the e.s.r. spectra rather than obtain the principal values of the g and A tensors from the angular variation of the resonance positions [13] and hyperfine splittings [14] was based on three considerations. First there is only a limited range of orientations, particularly in the *ab* and *bc** planes, at which eight clearly resolved lines are observed. Secondly we wished to examine whether or not the occurrence of a small angle (12°) between the V–O vectors of the magnetically inequivalent molecules would lead to the simulation of two detectably separate spectra, one from each molecule, rather than the observed well resolved single spectrum. Thirdly, in the simulation of the e.s.r. spectra of the two-dimensional layered structures $[VOCl_2(tmu)_2]$ and $[H_2tmen][VO(mal)_2(H_2O)]\cdot 2H_2O$ the detailed shape of the simulated spectra was found to be very dependent on the linewidths employed. Thus $[VOCl_2(OPPh_3)_2]$ offered an excellent opportunity to examine the effects of linewidths on the spectra of a non-interacting system.

The simulations reproduce very well the total spectral width, the positions, and the relative intensities. However, it should be noted that we find that the Van Vleck truncated dipolar linewidth, ΔB_d, is always too small. We have found it necessary to supplement ΔB_d with an arbitrary extra linewidth, ΔB_m, which is different at different orientations of the molecules with respect to the applied magnetic field, see Table 1. The possibility that this requirement could be due to poor alignment was considered. With this in mind repeated realignments of the crystals were attempted without any improvement in the spectra. The other possibility was that the orientation of the magnetic field with respect to the *a* and *c** axes in the *ac** plane could be in error, since these positions do not necessarily coincide with maximum and minimum field positions. The orientations of the magnetic field finally used, *i.e.* (3,0), (13,0), *etc.*, were those which resulted in the best fit to the total spectral width, and to the magnetic field at the centre of the spectrum using the g and A parameters which gave good simulations of the spectra in the *ab* and *bc** planes. Any alterations of these orientations in the *ac** plane resulted in the experimental and calculated resonance fields and total widths being incompatible. One possible explanation for this extra linewidth parameter, ΔB_m, is that it may reflect the presence of additional electronic exchange interaction between neighbouring molecules in the crystal lattice. Indeed, we have shown [8a] that the effect of a small (<50 G) electronic exchange on an e.s.r. simulation based upon a two-dimensional exchange interaction is to produce a 'monomeric' type of spectrum with no additional splitting of the hyperfine lines. In the case of $[VOCl_2(OPPh_3)_2]$ however, there is no one- or two-dimensional ordering in the crystalline lattice, so a corresponding simulation using a dimensional model is inappropriate.

The relative magnitudes of the hyperfine splittings and the linewidths at each orientation are in Table 1. These data, in conjunction with the simulated spectra in Figures 1—3, show that at the orientations where no features are resolved in the centre of the spectra [*viz.* (90, 70), (90, 80), and (90, 90) in the *ab* plane, and (80, 90) in the *bc** plane] the total width of an individual line is substantially larger than the effective hyperfine splitting. This results in broad overlapping hyperfine absorptions giving effectively a constant absorption, and hence a zero first derivative, over a wide range of magnetic fields. At other orientations the extent of resolution and the peak-to-peak height in the central region of the spectra are determined by the disparity between the linewidth and the hyperfine splitting. The smaller the linewidth compared to the hyperfine splitting the more nearly equal are the peak-to-peak heights of all the resonances.

The e.s.r. parameters used to obtain the simulated spectra were: $g_{xx} = g_{yy} = 1.974 \pm 0.002$, $g_{zz} = 1.930 \pm 0.002$, $A_{xx} = A_{yy} = -(66.1 \pm 2.8) \times 10^{-4}$ cm^{-1}, and $A_{zz} = -(175.0 \pm$

Table 1. Comparison of calculated hyperfine splittings and best-fit linewidths at various orientations of the magnetic field

η, γ	ΔB_d/ G	ΔB_m/ G	ΔB/ G	Effective hyperfine † splitting, A/G Molecule 1	Molecule 2
(*i*) *ab* Plane					
90, 0	63.2	20.1	83.3	73.8	73.8
90, 10	60.9	20.7	81.6	73.6	74.0
90, 20	55.1	22.4	77.5	73.2	74.0
90, 30	47.8	24.7	72.5	72.8	73.9
90, 40	42.3	27.5	69.8	72.4	73.7
90, 50	42.3	29.8	72.1	72.1	73.4
90, 60	47.7	32.0	79.7	71.8	73.0
90, 70	54.9	33.6	88.5	71.7	72.6
90, 80	60.4	34.7	95.1	71.8	72.2
90, 90	62.4	35.0	97.4	71.9	71.9
(*ii*) *bc** Plane					
90, 90	62.4	35.0	97.4	71.9	71.9
80, 90	62.1	34.9	97.0	75.6	80.2
70, 90	60.9	34.5	95.4	90.4	97.1
60, 90	58.9	33.8	92.7	110.0	117.5
50, 90	56.5	33.0	89.5	130.9	138.3
40, 90	53.8	32.2	86.0	150.7	157.2
30, 90	51.2	31.3	82.5	167.8	173.0
20, 90	49.0	30.6	79.6	181.0	184.7
10, 90	47.5	30.1	77.6	189.7	191.6
0, 90	46.9	29.9	76.8	193.3	193.3
(*iii*) *ac** Plane					
3, 0	46.5	30.0	76.5	193.9	
13, 0	48.0	29.9	77.9	192.7	
23, 0	54.0	29.3	83.3	186.2	
33, 0	62.1	28.2	90.3	174.9	
43, 0	69.6	6.8	76.4	159.3	
53, 0	74.5	5.1	79.6	140.5	
63, 0	75.7	13.4	89.1	119.7	
73, 0	73.3	11.8	85.1	99.0	
83, 0	67.8	10.6	78.4	81.5	
93, 0	61.2	5.0	66.2	72.2	
103, 0	55.7	25.2	80.9	75.2	
113, 0	53.3	31.1	84.4	88.9	
123, 0	54.0	42.5	96.5	108.4	
133, 0	56.1	44.2	100.3	129.5	
143, 0	57.3	46.0	103.3	149.5	
153, 0	56.4	27.5	83.9	167.0	
163, 0	53.2	28.7	81.9	180.7	
173, 0	49.0	29.6	78.6	189.9	
183, 0	46.5	30.0	76.5	193.9	

† Calculated from $g^2A^2 = g_{zz}^2A_{zz}^2\cos^2\theta + g_{xx}^2A_{xx}^2\sin^2\theta\cos^2\varphi + g_{yy}^2A_{yy}^2\sin^2\theta\sin^2\varphi$.

Table 2. Comparison of reported g and A values for some oxovanadium(IV) complexes

Compound	$g_{\parallel}$	$g_{\perp}$	$10^4A_{\parallel}$/ cm^{-1}	$10^4A_{\perp}$/ cm^{-1}	Ref.
$[VOCl_2(OPPh_3)_2]$	1.930 ±0.002	1.974 ±0.002	−175.0	−66.1	This work
$[VOCl_2(tmu)_2]$	1.941 ±0.003	1.983 ±0.003	−174.9	−64.1	16
$[VOCl_4]^{2-}$	1.948	1.979	−168.8	−62.8	17
$[VOF_4]^{2-}$	1.932	1.972	−180.0	−67.2	18
$[VO(pbd)_2]$	1.943 ±0.001	1.982 ±0.001	−170.0	−70.0	7

Table 3. Calculated m.o. coefficients for $[VOCl_2(OPPh_3)_2]$, using fixed values of ζ_V[25] and P[15] appropriate to the same oxidation state

$(N_2')^2$	$(N_3')^2$	β'	δ	γ_3	γ	$(N_4')^2$	K
(i) Assuming ζ_V = 250 cm^{-1} and P = 172 × 10^{-4} cm^{-1} [a]							
0.983	0.664	0.132	0.356	0.9	0.266	0.512	0.837
				0.8	0.199	0.582	
				0.7	0.142	0.653	
				0.6	0.093	0.726	
				0.5	0.052	0.797	
(ii) Assuming ζ_V = 210 cm^{-1} and P = 150 × 10^{-4} cm^{-1} [b]							
0.923	0.772	0.145	0.272	0.9	0.391	0.473	0.833
				0.8	0.285	0.555	
				0.7	0.201	0.637	
				0.6	0.133	0.717	
				0.5	0.079	0.792	
(iii) Assuming ζ_V = 170 cm^{-1} and P = 128 × 10^{-4} cm^{-1} [c]							
0.885	0.918	0.180	0.150	0.5 [d]	0.218	0.743	0.828
				0.4	0.104	0.846	
				0.3	0.039	0.915	

[a] The single-electron spin–orbit coupling constant for V^{4+}, and the value of P corresponding to an effective charge of +4 on the V atom. [b] The single-electron spin–orbit coupling constant for V^{3+}, and the value of P corresponding to an effective charge of +3 on the V atom. [c] Single-electron spin–orbit coupling constant for V^{2+}, and the value of P corresponding to an effective charge of +2 on the V atom. [d] Values of $\gamma_3 > 0.5$ gave complex values of γ and N_4' and were thus ignored.

2.8) × 10^{-4} cm^{-1}. The negative sign of the hyperfine splitting constants arises, in part, from the positive sign of the nuclear g value for ^{51}V, which contributes to the isotropic part of the hyperfine splitting constant.[15]

The largest discrepancy between the experimental and calculated magnetic fields at the spectrum centre is 21 G (in 12 750 G) for the (133, 0) orientation in the ac^* plane. The majority of the other orientations agree to within 10 G, which is the approximate error in measuring the magnetic field directly from the spectrum. Table 2 compares the g and A values obtained for $[VOCl_2(OPPh_3)_2]$ with some previously reported values for other oxovanadium(IV) complexes. It may be seen that, whilst the A values for the various compounds are approximately constant, the $g_{\parallel}$ value for $[VOCl_2(OPPh_3)_2]$ is significantly lower than the reported value for the other compounds containing chlorine and/or oxygen donor ligands, and indeed is almost identical to the $g_{\parallel}$ value for $[VOF_4]^{2-}$.

Molecular-orbital (m.o.) Calculations for $[VOCl_2(OPPh_3)_2]$. —A number of m.o. calculations have been performed [16–23] with the aim of investigating the bonding in various oxovanadium(IV) compounds. These have mainly concentrated upon correlating the spin-Hamiltonian parameters obtained from e.s.r. spectroscopy with the electronic structure of the oxovanadium(IV) complex.

Table 4. Calculated m.o. coefficients for $[VOCl_2(OPPh_3)_2]$, using ζ_V = 250 cm^{-1} and various values of P

$(N_2')^2$	$(N_3')^2$	β'	δ	γ_3	γ	(N_4')	K
(i) Assuming P = 160 × 10^{-4} cm^{-1} [a]							
0.901	0.719	0.166	0.313	0.9	0.248	0.517	0.835
				0.8	0.176	0.586	
				0.7	0.114	0.659	
				0.6	0.062	0.731	
				0.5	0.019	0.799	
(ii) Assuming P = 150 × 10^{-4} cm^{-1} [b]							
0.860	0.772	0.202	0.272	0.9	0.235	0.521	0.833
				0.8	0.153	0.593	
				0.7	0.086	0.665	
				0.6	0.030	0.734	
(iii) Assuming P = 140 × 10^{-4} cm^{-1} [c]							
0.803	0.833	0.248	0.224	0.9	0.221	0.524	0.831
				0.8	0.124	0.599	
				0.7	0.047	0.669	
(iv) Assuming P = 128 × 10^{-4} cm^{-1} [d]							
0.694	0.918	0.332	0.150	0.9	0.233	0.521	0.828
				0.8	0.075	0.606	
(v) Assuming P = 118.2 × 10^{-4} cm^{-1} [e]							
0.435	1 [f]	0.570	0	0.8	0.121	0.599	0.827
				0.7	0.299	0.599	

[a] Corresponding to an effective charge of *ca.* +3.5 on the V atom. [b] Corresponding to an effective charge of +3 on the V atom. [c] Corresponding to an effective charge of *ca.* +2.5 on the V atom. [d] Corresponding to an effective charge of +2 on the V atom. [e] Calculated using $N_3' = 1$ and $\delta = 0$. This value of P corresponds to a charge of $< +2$ on the V atom. [f] Assumed value of N' from which P was calculated.

The method used here for the m.o. calculations follows that described by Garner *et al.*[24] for the $[CrOCl_4]^-$ anion. Because of the axially symmetric spin-Hamiltonian parameters we assume that $[VOCl_2(OPPh_3)_2]$ has effectively C_{4v} symmetry, and that the m.o. coefficients of the chlorine and $OPPh_3$ ligands are not substantially different.

Assuming a b_2^* ground term, the perturbation expressions (5)—(8) may be derived relating the g and A values to the

$$g_{\parallel} = 2.0023 - N_2'N_3'A(8 - 16\delta\beta^1) \quad (5)$$

$$g_{\perp} = 2.0023 - N_3'N_4'D(4 + 8\gamma\delta) \quad (6)$$

$$A_{\parallel}/P = -\tfrac{4}{7}(N_3')^2 - K(N_3')^2 + (g_{\parallel} - 2.0023 - 16\delta\beta^1AN_2'N_3^1 - \tfrac{3}{7}(2.0023 - g_{\perp} - 8\gamma\delta DN_3'N_4') \quad (7)$$

$$A_{\perp}/P = \tfrac{2}{7}(N_3')^2 - K(N_3')^2 - \tfrac{11}{14}(2.0023 - g_{\perp}) + 32N_3'N_4'D\gamma\delta \quad (8)$$

electronic structure,[24] where the parameters N_i' are the metal d-orbital coefficients in the antibonding m.o.s as defined in ref. 24 and where A, D, and P are defined in equations (9)—(11). Here ζ_V, ζ_{Cl}, and ζ_O are single electron

$$A = \frac{N_2'N_3'}{\Delta E_{x^2-y^2}} \cdot [\zeta_V - (\zeta_{Cl} + \zeta_O)\delta\beta'] \quad (9)$$

$$D = \frac{N_3'N_4'}{2\Delta E_{xz}} \cdot [\zeta_V - (\zeta_{Cl} + \zeta_O)\delta\gamma] \quad (10)$$

$$P = 2g_N\beta\beta_N\langle r^{-3}\rangle \quad (11)$$

Table 5. Comparison of calculated m.o. coefficients for VO^{2+} complexes

Compound	ζ/cm^{-1}	10^4P/cm^{-1}	$(N_2')^2$	$(N_3')^2$	$(N_4')^2$	Ref.
$[VOCl_2(OPPh_3)_2]$	250	128.0	0.694	0.918	0.521	This work
	250	118.2	0.435	1 [a]	0.599	This work
	170	128.0	0.885	0.918	0.743	This work
[VO(salen)]	248	116.1	0.386	1 [a]	0.430	22
[VO(acen)]	248	111.4	0.356	1 [a]	0.440	22
$[VO(H_2O)_5]^{2+}$	135	174	0.962	1 [a]	0.925	23
$[VOCl_5]^{3-}$	135	174	<1	<1	0.99	23
$[VOF_4]^{2-}$			0.760	0.915	0.803	18 [b]
$[VOCl_4]^{2-}$			0.688	0.915	0.780	18 [b]
$[VO(pfp)_2]^{2-}$	248	128	0.45	0.92	1	26
	248	108	0.38	1	0.9	26

[a] Assumed value. [b] SCF-MS-Xα calculations. salen = *N*,*N*'-Ethylenebis(salicylideneiminate); acen = *N*,*N*'-ethylenebis(acetylacetonylideneiminate).

spin–orbit coupling constants for the vanadium 3*d*, chlorine 3*p*, and oxygen 2*p* orbitals respectively, $\Delta E_{x^2-y^2}$ and ΔE_{xz} are the electronic excitation energies for the $3d_{xy} \rightarrow 3d_{x^2-y^2}$ and $3d_{xy} \rightarrow 3d_{xz}$ transitions respectively, β' is a measure of the in-plane ligand σ bonding to the vanadium $3d_{x^2-y^2}$ orbital, δ and γ are measures of the π bonding from the in-plane ligands to the vanadium $3d_{xy}$ and $3d_{xz}$ orbitals respectively, and *K* is the isotropic Fermi contact parameter.

In order to calculate the m.o. coefficients the ΔE values were taken from ref. 4 and the following procedures were adopted. (*i*) For an initial calculation, terms in β', δ, or γ in equations (7) and (8) were ignored and a value of *P* assumed. This allowed values for N'_3 and δ to be found by solving these equations and making use of the normalisation condition in equation (12). (*ii*) Substituting these values for $N_3'\delta$ in equations (5) and (9) allowed values of $N_2'\beta'$ to be deduced with the assistance of the normalisation condition in equation (13). (*iii*) Since the normalisation condition of the e_1* orbital [equation (14), γ_3 is a measure of the terminal oxygen π bonding to the vanadium $3d_{xz}$ or $3d_{yz}$ orbitals] contained three unknowns, *i.e.* N_4', γ, and γ_3, it was

$$(N_3')^2(1 + 4\delta^2) = 1 \quad (12)$$

$$(N_2')^2(1 + 4\beta'^2) = 1 \quad (13)$$

$$(N_4')^2(1 + 2\gamma^2 + \gamma_3^2) = 1 \quad (14)$$

decided to calculate N_4' and γ for a range of fixed values of γ_3 after substituting for N_3' and δ in equations (6) and (10).

The m.o. coefficients were calculated using the tabulated free-ion values for the single-electron vanadium spin–orbit coupling constants [25] for V^{4+}, V^{3+}, and V^{2+} and the corresponding free-ion values of *P* for V^{4+}, V^{3+}, and V^{2+}.[15] The results of these calculations are in Table 3. Molecular-orbital coefficients were also calculated by keeping ζ_V constant at the free-ion value of V^{4+}, and varying *P*. These results are in Table 4, along with two calculations where N_3' was assumed to be unity. Throughout the calculations the values of the chlorine 3*p* and oxygen 2*p* spin–orbit coupling constants were fixed at 586 and 151 cm^{-1} respectively.[11]

The results in Tables 3 and 4 show, as noted previously,[24,26,27] that the derived m.o. coefficients are dependent on the assumptions used. However, the range may be restricted if we assume that it is unreasonable for the metal contribution to b_1* to be greater than that to b_2*, *i.e.* $N_2' > N_3'$. When no assumptions are made concerning the value of N_3' reasonable values of the m.o. coefficients were obtained for $P \leqslant 140$ 10^{-4} cm^{-1} with $\zeta_V = 250$ cm^{-1}. These values correspond to effective charges on the vanadium of $\leqslant -2.5$ and $+4$ respectively. If we assume that only values of *P* and ζ_V relevant to the same charge should be used in combination, then the above criterion is only satisfied for a charge on the vanadium of $\leqslant +2$. When $N_3' = 1$, *i.e.* $3d_{xy}$ is totally non-bonding, the calculated value of *P*, for ζ_V equal to the free-ion value for V^{4+}, corresponds to a charge of $< +2$ on the vanadium.

A comparison of the metal contribution to the various molecular orbitals derived in this and other work is given in Table 5. The wide disparity between many of the m.o. coefficients is probably as indicative of the variety of assumptions made in the calculations as of the change in ligands. Calculations which assume $N_3' = 1$ [22,23,27] are probably the least realistic even when overlap integrals are included in the calculations. As we have found, Bramman *et al.*[27] also concluded that m.o. coefficients for $[VO(pfp)_2]^{2-}$, where pfp = perfluoropinacolate(2−) (perfluoro-2,3-dimethylbutane-2,3-dionate), were only acceptable for values of *P* corresponding to V^{2+} or V^+ when $\zeta_V = 250$ cm^{-1}. Recent SCF-MS-Xα calculations [18] on $[VOCl_4]^{2-}$ gave m.o. coefficients independently of experimental data, see Table 5. These calculations have been used subsequently to calculate the e.s.r. parameters, which were in good agreement with experiment.[28] In this latter work the calculated values of ζ_V and of *P* were 209 cm^{-1} and 123×10^{-4} cm^{-1} respectively. There appears to be reasonably good agreement between the SCF-MS-Xα calculated parameters and those found in the present work, although we tend to underestimate the metal contribution to the e* orbitals compared with the SCF-MS-Xα calculation.

Acknowledgements

We thank S.E.R.C. for financial support. Computations were performed at the University of Manchester Regional Computer Centre on the ICL 1900/CDC 7600 Joint System.

References

1 A. Abragam and B. Bleaney, ' Electron Paramagnetic Resonance of Transition Metal Ions,' Oxford University Press, London, 1970.
2 R. L. Belford, N. D. Chasteen, H. So, and R. E. Tapscott, *J. Am. Chem. Soc.*, 1969, **91**, 4675.
3 D. M. S. Bagguley and J. H. E. Griffiths, *Proc. R. Soc. London, Ser. A*, 1950, **201**, 366.
4 D. Collison, B. Gahan, C. D. Garner, and F. E. Mabbs, *J. Chem. Soc., Dalton Trans.*, 1980, 667.
5 H. A. Kuska and M. T. Rogers, in ' Radical Ions,' eds. E. T. Kaiser and L. Kevan, Interscience, New York, 1959, pp. 579—745.
6 M. A. Hitchman and R. L. Belford, *Inorg. Chem.*, 1969, **8**, 958; R. L. Belford, D. T. Huang, and H. So, *Chem. Phys. Lett.*, 1972,

14, 592; F. Kubec and Z. Sroubek, *J. Chem. Phys.*, 1972, **57**, 1660; P. W. Lau and W. C. Lin, *ibid.*, 1973, **59**, 3988; D. P. Madaczi, R. H. Bartram, and O. R. Gilliam, *Phys. Rev. B*, 1973, **7**, 1817.
7 G. D. Simpson, R. L. Belford, and G. Biagioni, *Inorg. Chem.*, 1978, **17**, 2424.
8 (*a*) D. Collison, B. Gahan, and F. E. Mabbs, preceding paper; (*b*)B. Gahan and F. E. Mabbs, *J. Chem. Soc., Dalton Trans.*, 1983, 1695.
9 C. D. Garner, P. Lambert, F. E. Mabbs, and J. K. Porter, *J. Chem. Soc., Dalton Trans.*, 1972, 30.
10 M. R. Caira and B. J. Gellatly, *Acta Crystallogr., Sect. B*, 1980, **36**, 1198.
11 A. Carrington and A. D. MacLachlan, 'Introduction to Magnetic Resonance,' Harper and Row, London, 1967.
12 J. H. Van Vleck, *Phys. Rev.*, 1948, **74**, 1168.
13 D. S. Schonland, *Proc. Phys. Soc. London*, 1959, **73**, 788.
14 A. Lund and T. Vanngard, *J. Chem. Phys.*, 1965, **42**, 2979.
15 B. R. McGarvey, *J. Phys. Chem.*, 1967, **71**, 51.
16 H. A. Kuska and P.-H. Yang, *Inorg. Chem.*, 1974, **13**, 1090.
17 J. M. Flowers, J. C. Hempel, W. E. Hatfield, and H. H. Dearman, *J. Chem. Phys.*, 1973, **58**, 1479.
18 K. K. Sunil and M. T. Rogers, *Inorg. Chem.*, 1981, **20**, 3283.
19 C. J. Ballhausen and H. B. Gray, *Inorg. Chem.*, 1962, **1**, 111.
20 P. T. Manohran and M. T. Rogers, *J. Chem. Phys.*, 1968, **49**, 5510.
21 A. Jezierski and B. J. Raynor, *J. Chem. Soc., Dalton Trans.*, 1981, 1.
22 K. P. Callahan and P. J. Durand, *Inorg. Chem.*, 1980, **19**, 3211.
23 K. De Armond, B. B. Garrett, and H. S. Gutouski, *J. Chem. Phys.*, 1965, **42**, 1019.
24 C. D. Garner, I. H. Hillier, F. E. Mabbs, C. Taylor, and M. F. Guest, *J. Chem. Soc., Dalton Trans.*, 1976, 2258.
25 B. N. Figgis and J. Lewis, *Prog. Inorg. Chem.*, 1964, **6**, 37; T. M. Dunn, *Trans. Faraday Soc.*, 1961, **57**, 1441.
26 J. T. C. Van Kemenade, *Rec. Trav. Chim. Pays-Bas*, 1973, **92**, 1102.
27 P. F. Bramman, T. Land, J. B. Raynor, and C. J. Willis, *J. Chem. Soc., Dalton Trans.*, 1975, 45.
28 K. K. Sunil, J. F. Harrison, and M. T. Rogers, *J. Chem. Phys.*, 1982, **76**, 3087.

Received 4*th October* 1982; *Paper* 2/1710